

## Experiment 4: Modeling and Control of a Magnetic Levitation System

**Concepts emphasized:** Dynamic modeling, time-domain analysis, PI and PID feedback control.

### 1. Introduction

Magnetic levitation is becoming widely applicable in magnetic bearings, high-speed ground transportation, vibration isolation, etc., [1]. For example, magnetic bearings support radial and thrust loads in rotating machinery. In addition, magnetic suspension generates levitation action in rectilinear motion devices such as high-speed ground transportation systems. Magnetic levitation is immensely beneficial in the aforementioned rotary and rectilinear devices as it yields a non-contact support, without lubrication, thus eliminating friction. All practical magnetic levitation systems are inherently open-loop unstable and rely on feedback control for producing the desired levitation action.

The “maglev” experiment is a magnetic ball suspension system which is used to levitate a steel ball in air by the electromagnetic force generated by an electromagnet. The maglev system consists of an electromagnet, a ball rest, a ball position sensor, and a steel ball. The maglev system is completely encased in a rectangular enclosure divided into three distinct vertical chambers. The upper chamber houses an electromagnet such that one pole of the electromagnet is exposed to the middle chamber and faces a black post erect in the middle chamber. The post is designed such that with a 2.54 cm steel ball at rest on its surface, the top of the ball surface is 14 mm from the face of the electromagnet. The middle chamber is illuminated using a light bulb. The ball elevation from the top face of the post is measured using a sensor embedded in the post. The bottom chamber houses sensor circuitry for signal conditioning.

The objective of the experiment is to design a controller that levitates the steel ball from the post and makes it track a specified position trajectory. The maglev system can be decomposed into two subsystems, *viz.*, a mechanical subsystem and an electrical subsystem (current loop). The ball position in the mechanical subsystem can be controlled by adjusting the current through the electromagnet whereas the current through the electromagnet in the electrical subsystem can be controlled by applying controlled voltage across the electromagnet terminals. Thus, the voltage

applied across the electromagnet terminals provides an indirect control of the ball position.

In this laboratory exercise, we will first develop the governing differential equation and the Laplace domain transfer function models of the electrical and mechanical subsystems. Next, we will design and implement a proportional-integral (PI) controller to guarantee that the electrical subsystem current response tracks the specified current command. Finally, we will design and implement a proportional-integral-derivative (PID) controller to ensure that the mechanical subsystem ball position response tracks the desired position command.

## 2. Background

**Electrical Subsystem Modeling:** A schematic representation of the **maglev ideal electrical subsystem** is given in Figure 1. The electromagnet coil has an **inductance  $L$**  (Henry) and a **resistance  $R_\ell$**  (Ohm). The voltage  $V$  applied to the coil results in a current  $i$  governed by the differential equation [3]

$$V = iR_\ell + L \frac{di}{dt}. \quad (2.1)$$

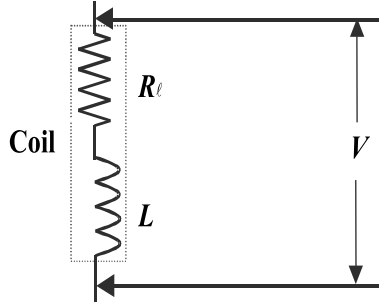


**Figure 1:** Ideal Electrical System

In order to **determine the current in the coil**, the mglev actual electrical subsystem (see Figure 2) is equipped with a resistor  **$R_s$  in series** with the coil such that the voltage  $V_s$  across  $R_s$  can be measured using an A/D converter. Now, the **voltage  $V_s$  measured across  $R_s$  can be used to compute the current  $i$  in the coil**. Note that with the sensing resistor  $R_s$  in the circuit the governing differential equation for the coil current becomes

$$V = i(R_\ell + R_s) + L \frac{di}{dt}. \quad (2.2)$$

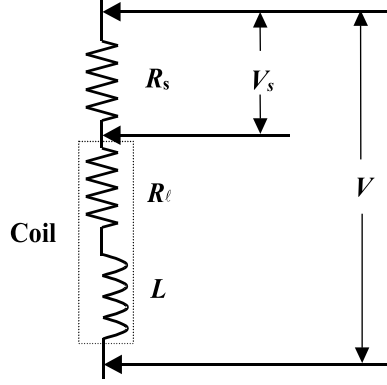


**Figure 2:** Actual Electrical System

Finally, taking the Laplace transform of (2.2), we obtain

$$G_e(s) \triangleq \frac{I(s)}{V(s)} = \frac{1}{Ls + (R_\ell + R_s)}, \quad (2.3)$$

where  $I(s) \triangleq \mathcal{L}[i(t)]$  and  $V(s) \triangleq \mathcal{L}[V(t)]$  and  $\mathcal{L}$  is the Laplace operator.

**Mechanical Subsystem Modeling:** The force experienced by the ball under the influence of electromagnet is given by [2, 3]

$$F = mg - K_f \left( \frac{i}{x} \right)^2, \quad (2.4)$$

where  $i$  is the current in electromagnet (Ampere),  $x$  is the distance of the ball from the electromagnet face (mm),  $g$  is the gravitational constant ( $\frac{\text{mm}}{\text{sec}^2}$ ),  $K_f$  is the magnetic force constant for the electromagnet-ball pair, and  $m$  is the mass of the steel ball (Kg). Using Newton's second law, we now obtain the differential equation governing the ball position as

$$m \frac{d^2x}{dt^2} = mg - K_f \left( \frac{i}{x} \right)^2. \quad (2.5)$$

Note that using (2.5), we can compute the steady-state electromagnet coil current  $i_{ss}$  that produces the desired steady-state constant ball position  $x_{ss}$ . Specifically, setting  $\frac{d^2x}{dt^2} = 0$  in (2.5) yields

$$i_{ss} = \sqrt{\frac{mg}{K_f}} x_{ss}. \quad (2.6)$$

Now, theoretically one can use (2.6) to regulate the ball position. However, external disturbances, system parameter uncertainty/variation, etc., necessitate a feedback controller to improve the mechanical subsystem performance.

Next, defining a set of shifted variables

$$\hat{x}(t) \triangleq x(t) - x_{ss}, \quad (2.7)$$

$$\hat{i}(t) \triangleq i(t) - i_{ss}, \quad (2.8)$$

we can rewrite the dynamic equation (2.5), as

$$m \frac{d^2 \hat{x}}{dt^2} = mg - K_f \left( \frac{\hat{i} + i_{ss}}{\hat{x} + x_{ss}} \right)^2. \quad (2.9)$$

Now, linearizing (2.9) about  $(\hat{x} = 0, \hat{i} = 0)$ , yields [3]

$$\frac{d^2 \hat{x}}{dt^2} = \frac{1}{m} \left[ \frac{\partial}{\partial \hat{x}} \left( mg - K_f \frac{(\hat{i} + i_{ss})^2}{(\hat{x} + x_{ss})^2} \right) \Big|_{(\hat{x}=0, \hat{i}=0)} \hat{x} + \frac{\partial}{\partial \hat{i}} \left( mg - K_f \frac{(\hat{i} + i_{ss})^2}{(\hat{x} + x_{ss})^2} \right) \Big|_{(\hat{x}=0, \hat{i}=0)} \hat{i} \right], \quad (2.10)$$

or, equivalently,

$$\frac{d^2 \hat{x}}{dt^2} = \frac{2K_f i_{ss}^2}{x_{ss}^3 m} \hat{x} - \frac{2K_f i_{ss}}{x_{ss}^2 m} \hat{i}. \quad (2.11)$$

Finally, taking the Laplace transform of (2.11), we obtain

$$G_m(s) \triangleq \frac{\hat{X}(s)}{\hat{I}(s)} = -\frac{a}{s^2 - b}, \quad (2.12)$$

where  $\hat{X}(s) \triangleq \mathcal{L}[\hat{x}(t)]$ ,  $\hat{I}(s) \triangleq \mathcal{L}[\hat{i}(t)]$ , and

$$a \triangleq \frac{2K_f i_{ss}}{x_{ss}^2 m}, \quad b \triangleq \frac{2K_f i_{ss}^2}{x_{ss}^3 m}. \quad (2.13)$$

The numerical values of the electrical and mechanical subsystem parameters for the laboratory maglev model are provided in Table 1 below. In addition, the variables  $a$  and  $b$  in (2.13) are computed with  $x_{ss} = 7$  mm and  $i_{ss} = 1$  Amp.

### 3. Objective

- i) **PI control of the electrical subsystem** to track a desired current.
- ii) **PID control of the mechanical subsystem** to track a desired ball position.

Physical quantity	Symbol	Numerical value	Units
Coil inductance	$L$	0.4125	Henry
Coil resistance	$R_\ell$	10	Ohm
Current sensor resistance	$R_s$	1	Ohm
Force constant	$K_f$	32654	$\frac{\text{mN}\cdot\text{mm}^2}{\text{Amp}^2}$
Gravitational constant	$g$	9810	$\frac{\text{mm}}{\text{sec}^2}$
Ball mass	$m$	0.068	Kg

Table 1: Numerical Values for Physical Parameters of The Maglev System

## 4. Equipment List

- i)* PC with MultiQ-3 data acquisition card and connecting board
- ii)* Software environment: Windows, Matlab, Simulink, RTW, and WinCon
- iii)* Magnetic levitation apparatus with a steel ball
- iv)* Universal power module: UPM-2405
- v)* Set of leads

## 5. Experimental Procedure

- i)* Using the set of leads, universal power module, magnetic levitation apparatus, and the connecting board of the MultiQ-3 data acquisition card, complete the wiring diagram shown in Figure 3.
- ii)* Start Matlab and WinCon Server. In the Matlab window, at the command prompt, type “Experiment4” and hit the **Enter** key. This Matlab script will change the directory from the default Matlab directory to the directory where all files needed to perform Experiment 4 are stored.
- iii)* You can now perform various steps of the magnetic levitation control experiment. However, before proceeding, you **must** request your laboratory teaching assistant to check your electrical connections.
- iv)* From the **File** menu of the WinCon Server, select the option **Open** to load the experiment file “Experiment4\_A.wcp.” This will load the files for calibrating the ball sensor voltage

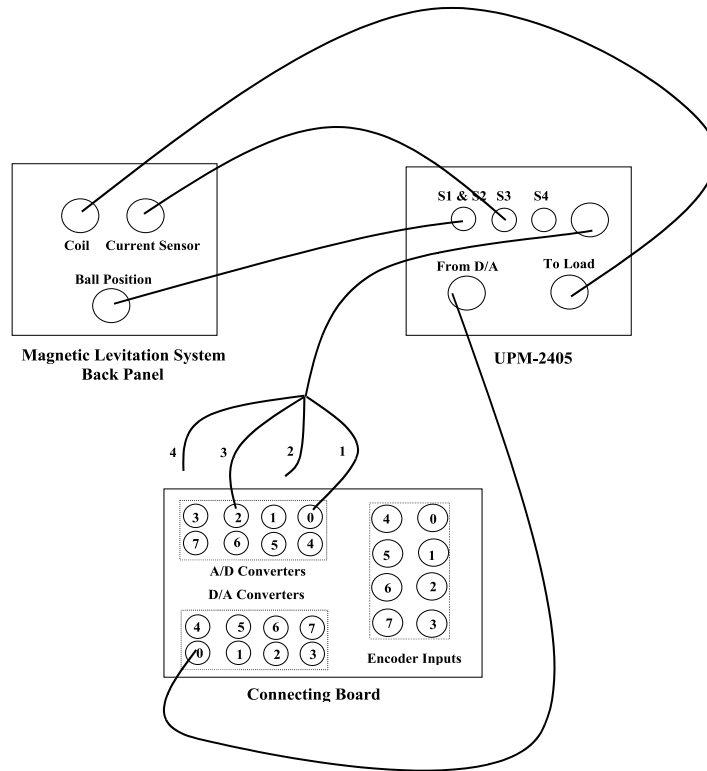


**Figure 3:** Wiring Diagram for The Maglev Experiment

when the ball is resting on the black post. The voltage measured on S1 should be about 0 Volts. A digital meter window will also appear on your desktop. Next, from the **Window** menu of the WinCon Server, select the option **Simulink**. This will load the Simulink block diagram “Experiment4\_A.mdl” shown in Figure 4 to your desktop.

- a) In the WinCon Server interface, click the green **Start** button to acquire the voltage measured on S1 (position sensor).
- b) Adjust the offset **potentiometer** on the Maglev to obtain 0 Volts.
- c) In the WinCon Server interface, click the red **Stop** button when you finish calibrating the sensor off-set.
- v) Close the currently opened digital meter window and the Simulink diagram. From the **File** menu of the WinCon Server, select the option **Open** to load the experiment file “Experiment4\_B.wcp.” This program applies 1.5 Amperes to the coil which causes the ball to jump up to the magnet and stay there. The voltage measured on S1 should be

between 4.75 and 4.95 Volts. A digital meter window will appear on your desktop. Next, from the **Window** menu of the WinCon Server, select the option **Simulink**. This will load the Simulink block-diagram “Experiment4\_B.mdl” shown in Figure 5 to your desktop.

- a) In the WinCon Server interface, click the green **Start** button to acquire the voltage measured on S1 (position sensor).

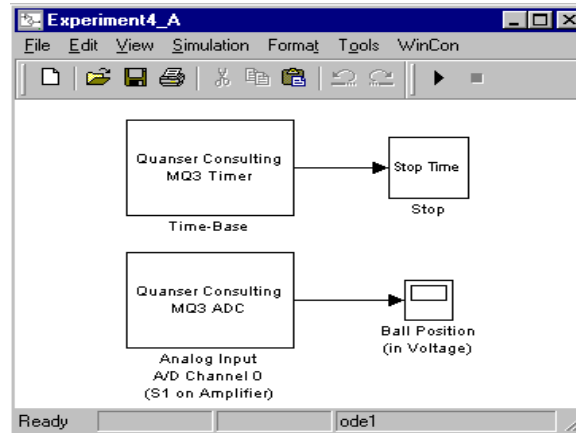


**Figure 4:** Simulink Block-Diagram for Ball Position Sensor Offset Calibration

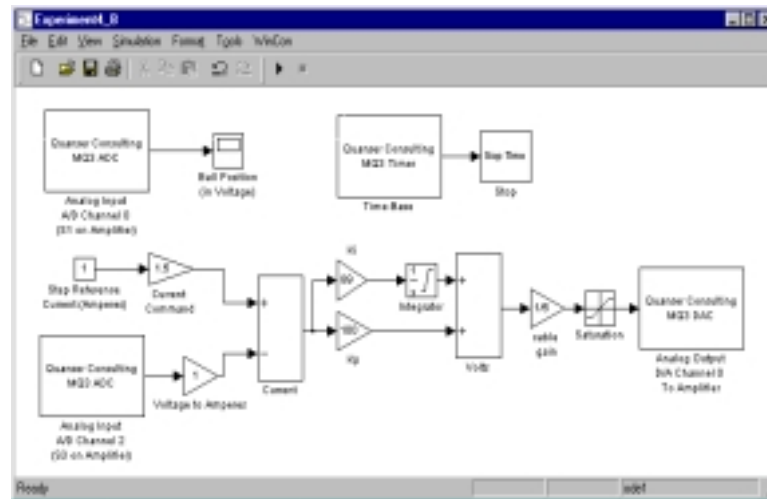


**Figure 5:** Simulink Block-Diagram for Ball Position Gain Calibration

- b) Adjust the gain **potentiometer** on the Maglev to obtain anywhere between **4.75 to 4.95** Volts on the position sensor.
  - c) In the WinCon Server interface, click the red **Stop** button when you finish calibrating the sensor gain.
- vi) Close the currently opened plot windows and the Simulink diagram. From the **File** menu of the WinCon Server, select the option **Open** to load the experiment file “Experiment4\_C.wcp.” A plot window will also appear on your desktop. Next, from the **Window** menu of the WinCon Server, select the option **Simulink** which loads the Simulink file “Experiment4\_C.mdl” shown in Figure 6 to your desktop. The various Simulink subblocks used in Figure 6 are given in detail in Figures 7–11.
  - a) In Figure 6, under the subblock labeled **Current Control** (Figure 10), the gains  $K_p$  and  $K_i$  must be designed and supplied by you. In particular, design a PI feedback controller so that the two poles of the close-loop electrical subsystem are -270 and -0.8 respectively. The feedback diagram of the electrical subsystem with the PI controller is shown in Figure 12, where  $A \triangleq R_\ell + R_s$ . The characteristic equation of the closed-loop system in Figure 12 can be used for the purpose of finding  $K_p$  and  $K_i$  such that the desired poles are achieved.
  - b) In Figure 6, under the subblock labeled **Mechanical control** (Figure 11), the gains  $K_p$ ,  $K_i$ , and  $K_d$  must also be designed and supplied by you. In particular, design a PID feedback controller so that the ball position step response exhibits a peak overshoot  $M_p \leq 5\%$  with settling time  $T_s \leq 0.19$  seconds. The close-loop system is a third order system; hence you must set the third pole to the left of the dominant complex-conjugate pole-pair. The feedback diagram of the mechanical subsystem with the PID controller is shown in Figure 13. The characteristic equation of the closed-loop system in Figure 13 can be used for the purpose of finding  $K_p$ ,  $K_i$ , and  $K_d$  such that the desired performance specifications are achieved. Note that in Figure 9, a feedforward controller based on (2.6) is also included to account for the  $i_{ss}$  term in (2.6).



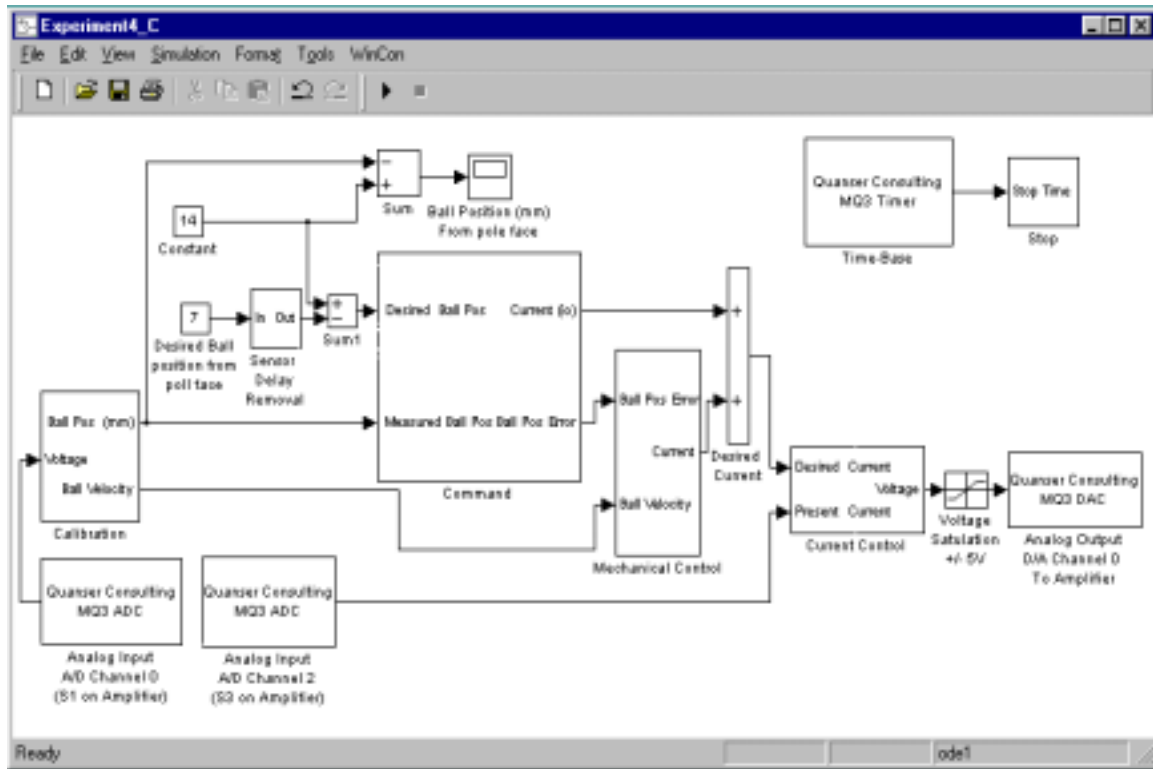


**Figure 6:** Simulink Block-Diagram for Magnetic Levitation System PID Controller

- c) Before proceeding, you **must** request your laboratory teaching assistant to approve your gain values. In the WinCon Server interface, click the green **Start** button to acquire the transient and steady-state position step response of the ball.

## 6. Analysis

- i) What is the significance of steps *iv)* and *v)* of Section 5 where we adjust the offset and gain potentiometers, respectively, to achieve the desired voltage from the position sensor?
- ii) Evaluate the actual overshoot and settling time of the ball position step response and compare with the specified overshoot and settling time. Comment.
- iii) How will the electrical subsystem (See Figure 12) respond if gains  $K_p$  and  $K_i$  are selected to set the two poles of the electrical subsystem at -1 and -0.8?

- iv) Can we experimentally set the real root of the closed-loop mechanical subsystem very far from the imaginary axis, in the left-half plane?

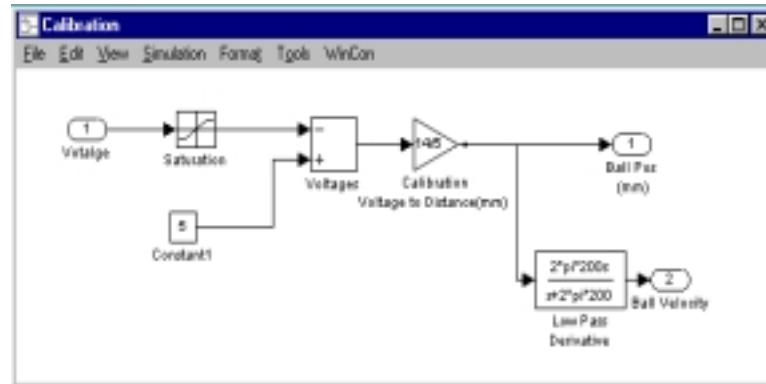


Figure 7: Calibration Subblock

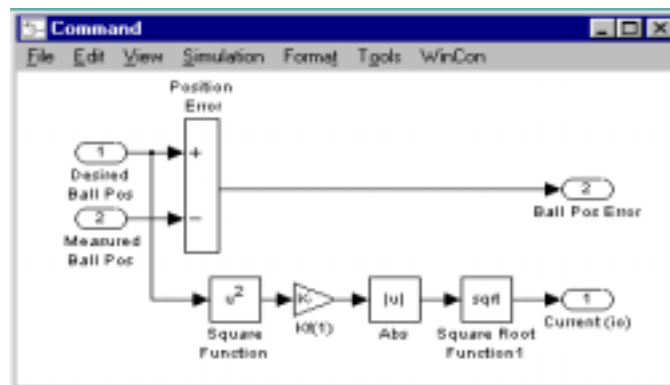


Figure 8: Command Subblock

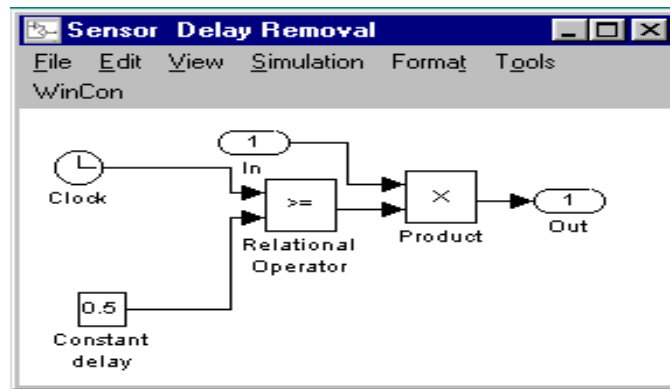


Figure 9: Sensor Delay Removal Subblock

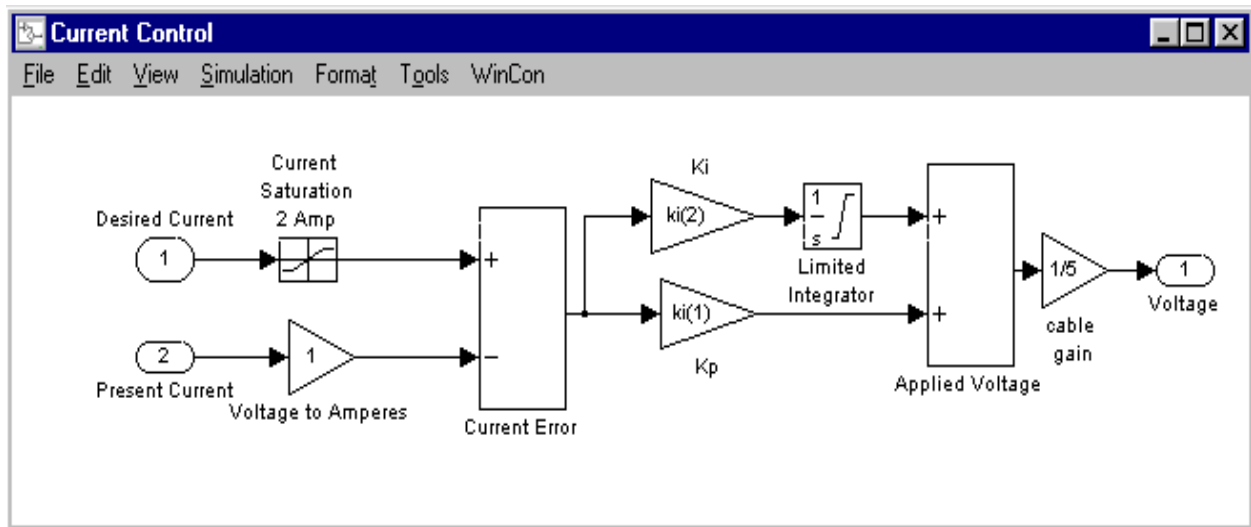
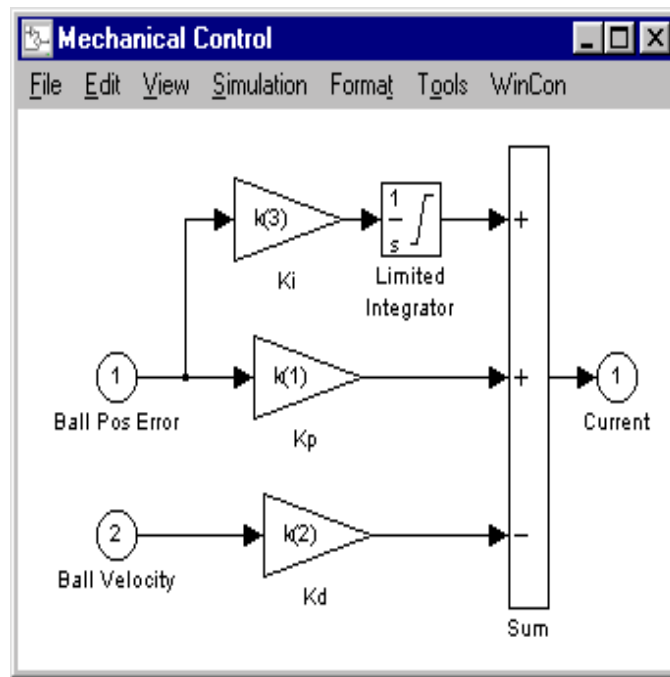
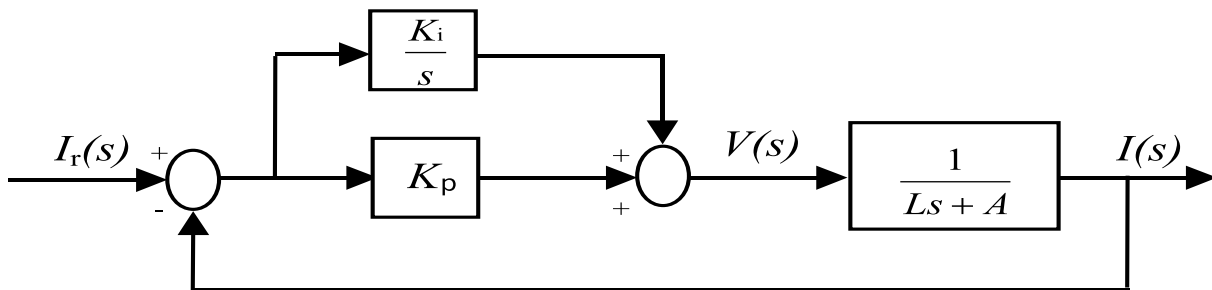


Figure 10: Current Control Subblock



**Figure 11:** Mechanical Control Subblock



**Figure 12:** Closed-Loop Feedback Interconnection for PI Control of Electrical Subsystem

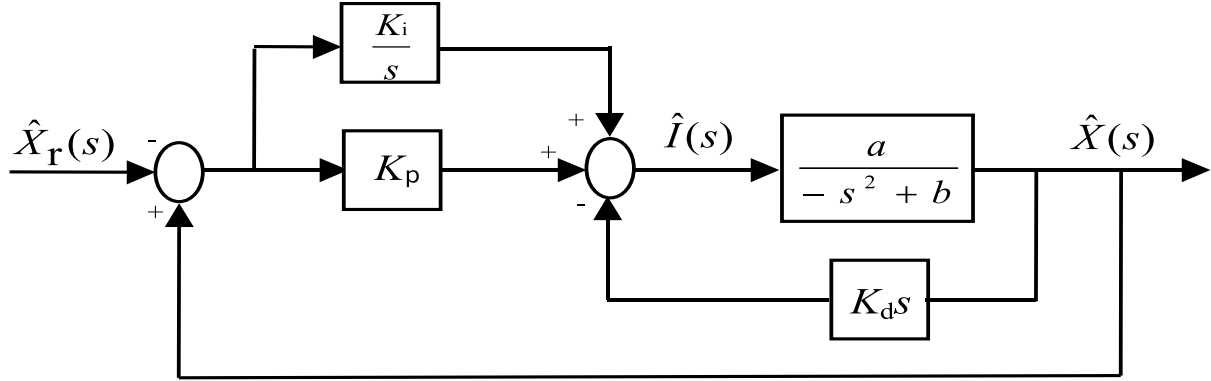


**Figure 13:** Closed-Loop Feedback Interconnection for PID Control of Mechanical Subsystem

## References

1. Special Issue on Magnetic Bearing Control, *IEEE Trans. Control System Technology*, 1996., Vol. 4, No. 5.
2. R. C. Dorf and R. H. Bishop, *Modern Control Systems*, Addison Wesley, Menlo Park, CA, 1998, 8<sup>th</sup> Ed., pp. 108.
3. B. Kuo, *Automatic Control Systems*, Prentice-Hall, Englewood Cliffs, NJ, 1995, 7<sup>th</sup> Ed., pp. 188–189.